

A GaAs MESFET Large-Signal Circuit Model for Nonlinear Analysis

M. Sango, O. Pitzalis, L. Lerner, C. McGuire, P. Wang, and W. Childs

EEsof, Inc., Westlake Village, CA 91362

ABSTRACT

A large-signal GaAs MESFET model for performing nonlinear microwave simulations with SPICE or Microwave SPICETM and LibraTM programs is described. The model includes accurate analytic representation of the dependence of gm , C_{gs} , C_{gd} , R_i , and R_{ds} upon operating voltages V_{gs} and V_{ds} . The model also functions as a master linear model that accurately replicates measured microwave s-parameters at arbitrarily chosen bias points within the transistor's useful operating I-V range. Microwave SPICE harmonic distortion simulations with the model compare favorably with measurements for an NEC NE71000. The model is useful in the analysis of a broad range of circuits including amplifiers, mixers, and oscillators.

INTRODUCTION

The simulation of harmonic generation and saturated gain effects in a GaAs MESFET requires a suitable large-signal circuit model for the transistor. Although there are a number of GaAs MESFET equivalent circuit models in current usage, none has proven to be fully satisfactory for accurate simulation of nonlinear GaAs MESFET operation. This paper describes a large-signal GaAs MESFET model that offers significant advancements over currently available popular models [1]-[3].

An effective and practical large-signal microwave GaAs MESFET model should satisfy the following objectives:

- 1) Provide an accurate representation of the measured DC I-V characteristics and assure convergence to steady-state conditions during time-domain transient analysis.
- 2) Provide an accurate representation of all the operating-point dependent nonlinearities that occur in large-signal operation.
- 3) Be supported by a practical characterization method for determining the model equivalent circuit parameters.

The large-signal GaAs MESFET model described in this paper, which builds upon the foundation provided by the modeling work of others [1]-[4], satisfies these objectives.

PART I: DESCRIPTION OF THE MODEL

The circuit topology for our model shown in Figure 1 is the same topology that has been widely accepted for the small-signal linear GaAs MESFET model but with the addition of the operating-point dependence of the nonlinear circuit elements and diode junction conductances so as to make the model valid in both large-signal as well as small-signal analyses. In the AC portion of the model there are five nonlinear circuit elements: gm , C_{gs} , C_{gd} , R_i , and R_{ds} , each of which varies as a function of V_{gs} and V_{ds} . However, the drain-to-gate capacitance, C_{gd} , is typically constant with V_{gs} and V_{ds} over a broad range corresponding to the region where I_{ds} saturation occurs. The model to be described accounts for the V_{gs} and V_{ds} dependence of gm , C_{gs} , C_{gd} , R_i and R_{ds} .

Other GaAs MESFET models account for the V_{gs} and V_{ds} dependence of gm only. The dependence of C_{gs} upon V_{gs} is modeled as the voltage dependence of a Schottky diode capacitance, but the V_{ds} dependence of C_{gs} is ignored. Also totally ignored in these models are the V_{gs} and V_{ds} nonlinearities in R_i and R_{ds} .

The following summarizes how the three modeling objectives have been addressed in the new model being described.

1) The modeling of the DC I-V characteristics:

A number of DC current-voltage relationships have been proposed for modeling the GaAs MESFET [1] [2] [3]. It is important for the DC equation to produce smooth functions free of discontinuities that could lead to non-convergence in non-linear simulators such as SPICE and Microwave SPICE. The DC equations chosen for this model are those recently proposed by Statz, et al. [3].

$$I_{ds} = \frac{\beta (V_{gs} - V_t)^2}{1 + b (V_{gs} - V_t)} (1 + \lambda V_{ds}) \tanh(\alpha V_{ds})$$

These equations give an accurate current and transconductance representation of the device with smooth continuous transitions at the threshold voltage important for convergence of time-domain analysis. Figure 2 shows the comparison between the measured and simulated DC I-V characteristics.

It is important to be aware that accurate DC I-V modeling is essential to accurate microwave simulation. For example, the V_{gs} , V_{ds} dependence of g_m is derived from the DC I-V curves. Also, accurate simulations of the onset of signal clipping output power saturation and harmonic generation associated with output power saturation, likewise depend upon accurate DC I-V modeling.

2) Accurate representation of all operating-point dependent nonlinearities that occur in large-signal operation:

We have derived analytical equations that model the operating-point dependence of the following elements: the gate charge (Q_g), the gate-source (C_{gs}) and gate-drain (C_{gd}) capacitances, the charging resistance (R_i), and the output resistance (R_{ds}).

In this model, nonlinear voltage-controlled current sources are used to replicate the bias dependence of R_i and R_{ds} . Previous formulations, both theoretical and empirical, had neglected the V_{ds} dependence of GaAs MESFET charges and capacitances. New expressions fully incorporate the dependence of Q_g , C_{gs} , and C_{gd} on both V_{gs} and V_{ds} biases. In addition, gate charge is conserved, and the capacitances C_{gs} and C_{gd} are continuous under all bias conditions.

The new equations lend themselves to easy implementation in nonlinear CAD systems, both for model parameter extraction as well as for nonlinear GaAs MESFET circuit simulations. Figures 3a through 3d compare the measured vs. modeled parameters C_{gs} , R_i , R_{ds} , and g_m using the new analytical expressions. The agreement between measurements and analytically calculated values is excellent for V_{ds} and V_{gs} covering the normal operating range of the transistor. The total V_{ds} dependence of C_{gs} and C_{gd} is modeled to follow the capacitance behavior of a symmetrical GaAs MESFET as shown in the curves of Figure 4.

The new model also serves as a master s-parameter model, capable of producing accurate s-parameters at arbitrarily specified DC bias points in the transistor operating region. This is an important requirement that any large-signal model must satisfy in order to be useful over the broadest range of circuit designs.

3) The Characterization Method:

The V_{gs} and V_{ds} dependence of the nonlinear circuit elements is determined using a procedure that begins with small-signal AC measurements. As a first step s-parameter measurements (typically to 26.5 GHz) are acquired at a series of V_{gs} , V_{ds} bias combinations spanning a broad operating point range for the transistor. This range typically covers V_{gs} steps from pinchoff to approximately +0.6 V for forward bias and steps of V_{ds} from zero to some voltage below breakdown. The fixed extrinsic resistances R_g , R_s , and R_d and the fixed external series inductances L_g , L_s , and L_d are extracted either through an optimized s-parameter model fit to the s-parameter data at a single V_{gs} , V_{ds} bias or through other DC and s-parameter measurement methods [6], [7]. At each bias and at a low frequency, typically a few hundred

megahertz, the s-parameter sets are next converted to y-parameter sets. Using the method proposed by Minasian [5], the intrinsic model circuit elements g_m , C_{gs} , C_{gd} , C_{ds} , R_{ds} , and τ are extracted at each V_{gs} , V_{ds} bias voltage set.

The remaining operating-point dependent model element R_i is determined through a straightforward optimization fit to S_{11} at each V_{gs} , V_{ds} combination. It is our experience that the best modeling fit for a broad range of commercial GaAs MESFETs occurs with the domain capacitance C_{dc} equal to zero. However, we have included C_{dc} in the model topology for completeness.

The procedural steps in modeling a GaAs MESFET are accomplished with automated data acquisition and data processing software that produces a data file for the large-signal model in four major steps:

- o First, the DC I-V characteristics of the device are acquired using an HP 4145B Semiconductor Parameter Analyzer.
- o Second, s-parameter measurements are taken over a limited range of bias, from which a modified Fukui technique and cold FET measurements are used to extract the extrinsic resistive and inductive contact parasitics of the MESFET. (Several other DC model parameters are also extracted from this step.)
- o Third, microwave s-parameters are acquired over a broad range of bias. Standard calibration and de-embedding techniques are used to correct the RF measurements taken in these steps. At each bias point, the intrinsic equivalent circuit parameters are extracted and stored.
- o Fourth, the large-signal model equations are fit to the extracted parameters at each V_{gs} , V_{ds} combination using gradient optimization.

PART II: MEASUREMENT-SIMULATION COMPARISONS

Harmonic-distortion measurements were made on an NEC NE71000 GaAs MESFET. The transistor chip was wire-bond interconnected within a microstrip to the coaxial test fixture. External coaxial bias tees were used to set the DC quiescent operating point at $V_{ds} = 4V$ and $I_{ds} = I_{ds}/2 = 25.3$ mA, corresponding to $V_{gs} = -0.36V$. An HP 8566 spectrum analyzer, used for measuring frequency selected power through the fifth harmonic also provided a known 50 Ohm load resistance at all frequencies. An HP 8642B signal generator was used for 2 GHz source drive that was varied from -40 dBm to +15 dBm. Simulations were performed using the new model and compared with the measurements. The bond wire inductances at the gate, source, and drain terminals of the NE71000 were included in the Microwave SPICE simulations.

Figure 5 shows the modeled I-V curves for the transistor with the 50 Ohm load line and quiescent operating point indicated. Figures 6a through 6e show plots of the measured and simulated data for each harmonic through the fifth. At the fundamental frequency there is excellent agreement at all power levels. The linear gain of 13.1 dB at 2 GHz is simulated exactly. The measured peak saturated output of 19.2 dBm differs from the simulation by less than 0.4 dB.

The simulations can be seen to closely replicate the measured data at each harmonic from the second through the fifth shown in Figs. 6b through 6e respectively.

PART III: CONCLUSIONS

A large-signal GaAs MESFET model for nonlinear analysis has been described. The model closely accounts for the operating-point dependent nonlinearities in the transistor as demonstrated through comparisons of measured with simulated distortion analyses.

The work represents a significant extension to previous large-signal modeling that is similar in concept [4]. The new contributions include:

- o The determination of analytic expressions that closely approximate the V_{gs} , V_{ds} dependence of the GaAs MESFET equivalent circuit elements G_m , C_{gs} , C_{gd} , R_i , and R_{ds} .
- o The development of a model that is accurate for reproducing measured GaAs MESFET s-parameters at arbitrarily selected bias points.
- o The development of a model that facilitates implementation in many nonlinear simulation programs.
- o Elimination of the convergence problems experienced in past models through advancements in continuity and charge conservation properties.
- o The provision for straightforward extraction of the model parameters by developing software to automate measurements, combined with data post processing to generate the model data file.

Microwave Spice and Libra are trademarks of EEsOf, Inc.

REFERENCES

- [1] W. R. Curtice, "A MESFET Model for Use in the Design of GaAs Integrated Circuits," *IEEE Trans. Microwave Theory Tech.*, MTT-28(5), pp. 448-56, May, 1980.
- [2] W. R. Curtice and M. Ettenberg, "A Nonlinear GaAs FET Model for Use in the Design of Output Circuits for Power Amplifiers," *IEEE Trans. Microwave Theory Tech.*, MTT-33, pp. 1383-94, Dec., 1985.
- [3] H. Statz, P. Newman, I.W. Smith, R. A. Pucel, H. A. Haus, "GaAs FET Device and Circuit

Simulation in SPICE," *IEEE Trans. Electron Devices*, Vol. ED-34, pp. 160-69, Feb., 1987.

- [4] H. A. Willing, C. Rauscher, P. de Santis, "A Technique for Predicting Large-Signal Performance of a GaAs MESFET," *IEEE Transactions on Microwave Theory and Techniques*, MTT-26(12), pp. 1017-1023, Dec., 1978.
- [5] R. A. Minasian, "Simplified GaAs MESFET Model to 10 GHz," *Electronics Letters*, Vol. 13, pp. 549-551, Sept., 1977.
- [6] H. Fukui, "Determinations of the Basic Parameters of a GaAs MESFET," *Bell Syst. Tech.*, J., Vol. 58, No. 3, March, 1979.
- [7] R. Vogel, "Determination of MESFET Resistive Parameters Using RF-Wafer Probing," Proc. 17th European Microwave Conference, Rome, Italy, pp. 616-621, 1987.

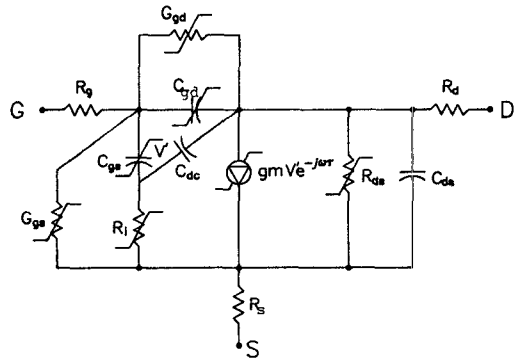


Figure 1: The equivalent circuit for the large-signal GaAs FET model.

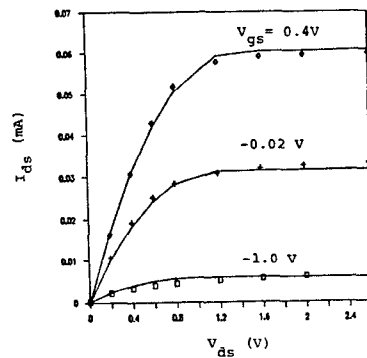


Figure 2: Comparison of measured (solid lines) and model simulations (markers) of the DC I-V characteristics of a GaAs MESFET.

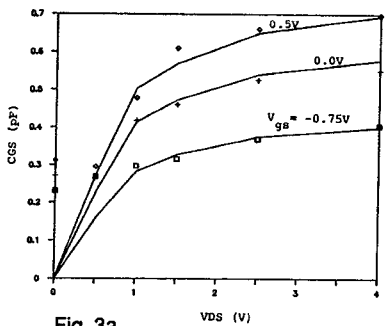


Fig. 3a

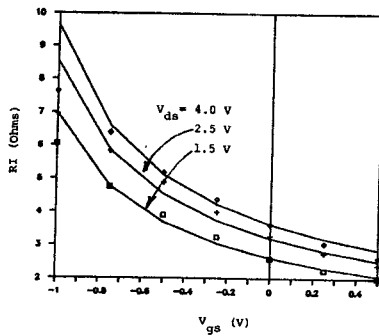
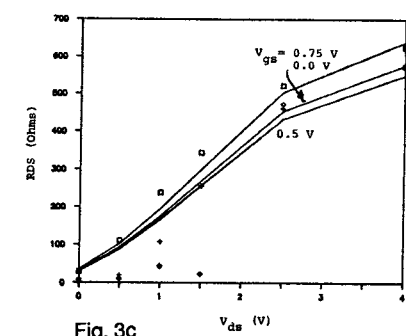


Fig. 3c



CGs AND CGD VS VDS

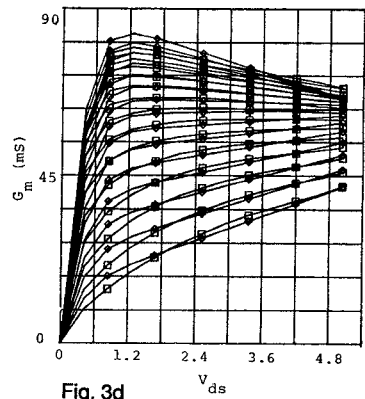


Fig. 3d

Figures 3a-3d: Comparison between measurement-derived (markers) and analytically fitted (solid lines) equivalent circuit elements as functions of V_{ds} and V_{gs} . (a) C_{gs} , (b) R_i , (c) R_{ds} , and (d) g_m .

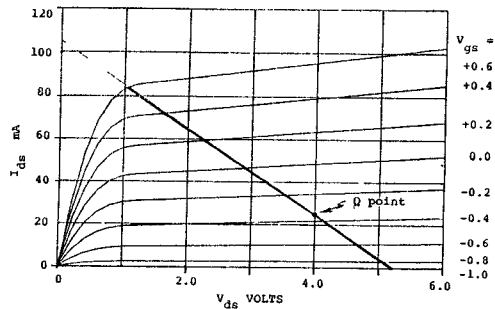


Figure 5: The simulated NE71000 I-V characteristics with 50 Ohm dynamic load line.

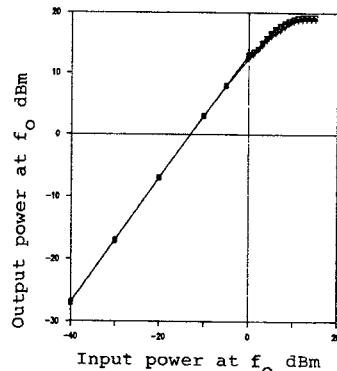


Fig. 6a: the fundamental frequency of f_0

Figure 4: The modeled C_{gs} and C_{gd} of the symmetrical MESFET for $V_{gs} = -0.25V$ and $V_{gs} = 0V$.

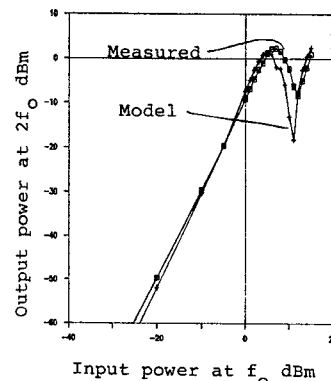


Fig. 6b: the second harmonic $2f_0$

Figures 6 (a) - (e): Results of power measurements and simulations of the NE71000.

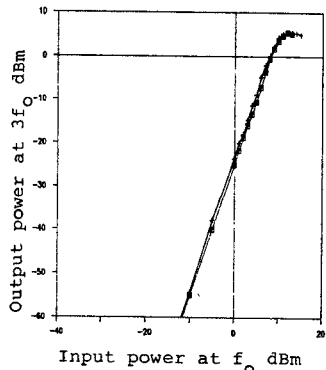


Fig. 6c: the third harmonic $3f_0$

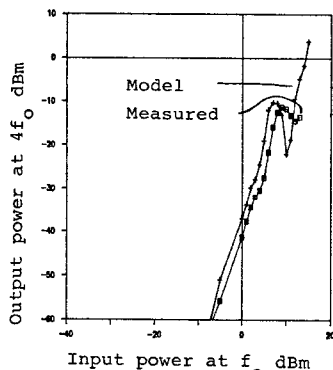


Fig. 6d: the fourth harmonic $4f_0$

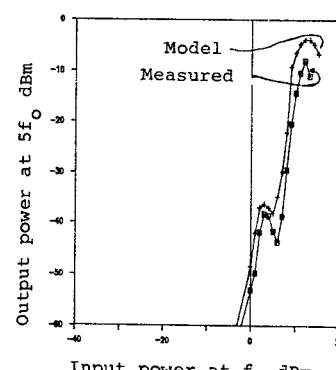


Fig. 6e: the fifth harmonic $5f_0$